NATIONAL ADVISORY COMMITTEE
FOR AERONAUTICS

TECHNICAL NOTE 2607

ELECTRICAL PRESSURE INTEGRATOR

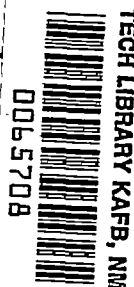By Arleigh P. Helfer

Langley Aeronautical Laboratory
Langley Field, Va.

NACA

Washington

January 1952

NATIONAL ADVISORY COMMITTEE FOR AERO̶̶̶̶̶̶̶̶̶̶

TECHNICAL NOTE 2607

ELECTRICAL PRESSURE INTEGRATOR

By Arleigh P. Helfer

SUMMARY

The design of an instrument utilizing Wheatstone bridge type of pressure sensing units that is capable of integration of airfoil pressures into a quantity representative of the normal force and pitching moment acting on the airfoil is presented. Subsequent division of the integrator output by dynamic pressure q results in normal-force and moment coefficients, c_n and c_m, without the need for lengthy manual integrations of manometer data. Flight and wind-tunnel versions of this instrument are briefly described along with samples of test data obtained from them. Design equations are presented and factors affecting instrument accuracy are discussed. The high accuracy and versatility of this instrument, accompanied by the large saving of time required for data reduction, renders it a very valuable research tool.

INTRODUCTION

The effort necessary to convert manually pressure data into force and moment coefficients has been a large hindrance in the application of the pressure technique for the acquisition of aerodynamic data. Brief periods of tunnel operation would produce pressure records that would saturate the computing section for extended periods and thus limit tunnel usefulness by regulating the rate at which data of this type could be presented. Flight testing, unfortunately, also experiences this same limitation. It thus became apparent that, with limited computer manpower available, a rapid and accurate means of obtaining force and moment coefficients was an essential prerequisite to the planning of programs of this type. Equipment described herein was designed to meet this need without a sacrifice in accuracy.

The function of pressure integrators may not be apparent. Thus, a brief review of the method of obtaining forces and moments on airfoil sections by the measurement of pressures may be in order. Normally there are from 30 to 44 pressure orifices including top and bottom at each spanwise location on an airfoil section, with as many spanwise locations as the available space and instrumentation permit. In order to obtain airfoil normal-force and moment coefficients c_n and c_m the records

of individual pressures are read, the pressures converted to pressure coefficients $\Delta p/q$, and a pressure-distribution diagram plotted. This pressure diagram is constructed by plotting $\Delta p/q$, with proper observation of sign, as the ordinate and the orifice location in percent chord as the abscissa. A typical pressure-distribution diagram is shown in figure 1. This diagram is then integrated with a planimeter type of integrator to obtain force and moment coefficients.

A number of instruments, which perform the complete job of measuring the pressures and integrating the results, have been designed. Probably the most familiar is the integrating multitube manometer. This instrument consists of a number of precision bore tubes, connected to a common sump, the level of which indicates the integration and is read on a glass indicating tube with a scale attached. Since all the precision bore tubes are usually of the same diameter, each tube contributes an equal amount to the total integrated value. In order to compensate for uneven orifice locations, several tubes are sometimes paralleled for one orifice. Another device consists of a metal beam and bellows arrangement with large bellows·on the ends connected to pressure regulators which keep the beam oriented in a horizontal position. The pressures in these bellows are measured with mercury manometers. Small bellows are connected to orifices in the top and bottom surfaces of the model and are spaced on the beam the same as the orifices on the model. If 50 percent chord is chosen as the center of moments, the actual moment is proportional to the difference of readings from the two end bellows and normal force is proportional to the sum. Both of these instruments operate satisfactorily but have not been used extensively because of the limitations they impose on orifice locations, their size and complexity, the need for precision parts, or their lack of adaptability to changing requirements in the research work. The electrical integrator to be described overcomes some but not all of these limitations. ·

The heart of the electrical instrument is a group of electrical pressure gages which convert the pressures to electrical voltages or currents. These gage outputs are properly modified or "weighted" for the locations and effective areas of orifices and then electrically added to give a single voltage or current proportional to the area in the pressure diagram. The result is normal force. This quantity is then used to indicate, print, or plot the final results. Moment is similarly obtained by considering moment arms along with effective areas of the orifices in the determination of the moment weighting. Thus, by proper choice of weighting factors an integrator can be used to measure either normal force or moment. Weighting of an integrator is a process of permitting each orifice to contribute to the total output, an amount dependent upon its percent-chord position and the area over which the pressure it measures is considered effective.

SYMBOLS

V	bridge supply voltage
E_O	output voltage
I	bridge output current
R	resistance of each bridge arm
ΔR	resistance change of each bridge arm due to load
R_d	voltage-dropping resistor
R_m	meter resistance
I_m	meter current
Z	circuit impedance
B	gage constant of proportionality relating pressure and bridge unbalance
W	weighting factor
P	pressure
F	total normal force
M	resulting moment
c_n	normal-force coefficient
c_m	moment coefficient
c	total airfoil chord
b	spanwise measurement
a	moment arm
q	dynamic pressure
J	propeller advance-diameter ratio

D   propeller diameter

v   tunnel speed

N   propeller rotational speed

A   constant of proportionality

·k   constant of proportionality

THEORY

Construction of an instrument of this type is realizable because of the unique fact that Wheatstone bridge outputs may be added algebraically by merely paralleling both input and output terminals of each in turn. Control is exercised over the percentage of the network output contributed by each bridge by dropping resistors in the voltage leads to regulate the input voltage to each bridge. When use is made of a sensing unit where bridge unbalance is proportional to pressure applied, the following analysis is a derivation of parallel bridge equations, the use of which converts the difficult problem of pressure integration to a relatively simple one of electrical current or voltage addition. By application of these equations a complete force and moment integrator can be designed and built.

Derivation of Bridge Summing Equations

In the usual four-active-arm direct-current Wheatstone bridge type of sensing circuit, as shown in figure 2, the current equation for small unbalances is defined by

$$I = \frac{V \, \Delta R}{R(R + R_m)} \tag{1}$$

If $V = k_1 x$ and $\frac{\Delta R}{R(R + R_m)} = k_2 y$, then $I = k_3 xy$ where $k_3 = k_1 k_2$, and x and y are independent variables. Thus, multiplication can be performed in a single bridge circuit by permitting the bridge voltage and bridge unbalance to vary as the quantities to be multiplied. Addition and subtraction is then performed by two or more bridges in parallel as shown in figure 3. While bridges of unequal resistances can be used, it is a more common practice to have all bridge arms R of the same resistance. The following analysis is made on this basis. In this circuit the

bridge voltage is supplied from a common voltage source V, individual
bridge voltages being determined by dropping resistors R_{d_1} and R_{d_2},
and the outputs are in parallel. When a sensitive microammeter is con-
nected across the combined output it reads the summation of the indi-
vidual bridge currents. The equivalent circuit of figure 3 is shown in
figure 4. With the use of Thévenins theorem, bridges 1 and 2 have been
replaced by their equivalent generators and series resistances. The
series resistance was determined by replacing the circuit of figure 5
with the equivalent Y-unit of figure 6 and solving for Z_1. As shown
in appendix A for small ΔR, the value of this quantity is R, the
resistance of one arm of the active bridge. Using superposition to solve
for meter currents I_2' and I_2'' in figures 7 and 8, respectively, the
total meter current is the sum of the currents due to each bridge no-load
output voltage acting in the composite circuit independently. Thus,

$$I_2 = I_2' + I_2'' \tag{2}$$

where I_2 is the total meter current. Use is made of this principle in
the practical computer to adjust bridge sensitivities to represent the
desired quantities. For the sake of simplicity, the desired sensitivities
were calculated as a certain ratio of the sensitivity of a standard bridge
and the currents were adjusted accordingly. Since the output current of
each bridge flows through a fixed resistance network (see appendix B),

$$I_2' = \frac{VX_1 \, \Delta R_1}{2R\left(\frac{R}{2} + R_m\right)} \tag{3}$$

$$I_2'' = \frac{VX_2 \, \Delta R_2}{2R\left(\frac{R}{2} + R_m\right)} \tag{4}$$

and

$$I_2 = \frac{V\left(X_1 \, \Delta R_1 + X_2 \, \Delta R_2\right)}{2R\left(\frac{R}{2} + R_m\right)} \tag{5}$$

where $X_1 = \dfrac{R}{R + R_{d_1}}$, $X_2 = \dfrac{R}{R + R_{d_2}}$, and R_{d_1} and R_{d_2} are the voltage-
dropping resistors of bridges 1 and 2, respectively, and ΔR_1 and ΔR_2
are their respective unbalances.

Additional bridges may be added to the preceding system to perform multiple-point integration. Thus, for a unit composed of n-bridges the output current through the meter circuit is given as

$$I_m = \frac{V\left(X_1 \, \Delta R_1 + X_2 \, \Delta R_2 + X_3 \, \Delta R_3 + \ldots X_n \, \Delta R_n\right)}{nR\left(\dfrac{R}{n} + R_m\right)} \tag{6}$$

If output voltage E_0, instead of current, is to be measured (that is, $R_m \longrightarrow \infty$), then

$$E_0 = \frac{V\left(X_1 \, \Delta R_1 + X_2 \, \Delta R_2 + X_3 \, \Delta R_3 + \ldots X_n \, \Delta R_n\right)}{nR} \tag{7}$$

Equations for Symmetrical Orifice Locations

The foregoing principle is useful in constructing pressure integrators from the Wheatstone bridge sensing unit. If the orifices on the upper airfoil surface are matched by an equal number of orifices on the lower surface located at the same percent-chord position as those on the upper surface, the orifice locations are considered symmetrical and a single differential pressure gage can be used for each pair of orifices. By permitting $\dfrac{\Delta R_1}{R} = B_1 \, \Delta P_1$, $\dfrac{\Delta R_2}{R} = B_2 \, \Delta P_2$, $\dfrac{\Delta R_3}{R} = B_3 \, \Delta P_3$, $\ldots \dfrac{\Delta R_n}{R} =$ $B_n \, \Delta P_n$, where ΔP_1, ΔP_2, ΔP_3, $\ldots \Delta P_n$ represents differential pressures existing across the airfoil at chordwise positions 1, 2, 3, $\ldots$ n and B_1, B_2, B_3, $\ldots B_n$ represents their respective constant of proportionality relating pressure and bridge unbalance, equation (6) becomes

$$I_m = \frac{V\left(X_1 B_1 \, \Delta P_1 + X_2 B_2 \, \Delta P_2 + X_3 B_3 \, \Delta P_3 + \ldots X_n B_n \, \Delta P_n\right)}{n\left(\dfrac{R}{n} + R_m\right)} \tag{8}$$

A more convenient form of equation (8) is

$$I_m = \frac{VB_x\left(\dfrac{X_1 B_1 \, \Delta P_1}{B_x} + \dfrac{X_2 B_2 \, \Delta P_1}{B_x} + \dfrac{X_3 B_3 \, \Delta P_3}{B_x} + \ldots \dfrac{X_n B_n \, \Delta P_n}{B_x}\right)}{n\left(\dfrac{R}{n} + R_m\right)} \tag{9}$$

where B_x is the constant of proportionality of the most insensitive

gage to be used in the integrator. Under these conditions, $\dfrac{B_1}{B_x}$, $\dfrac{B_2}{B_x}$, . . . $\dfrac{B_n}{B_x}$ is always equal to or greater than 1. In the practical integrator this procedure permits easy replacement of gages without the necessity of reweighting of the complete integrator. If this procedure is not followed and any gage is replaced with one having a sensitivity of less than B_x, complete integrator reweighting would then be necessary.

By equating $\dfrac{X_1 B_1}{B_x}$, $\dfrac{X_2 B_2}{B_x}$, $\dfrac{X_3 B_3}{B_x}$, . . . $\dfrac{X_n B_n}{B_x}$ equal to the weighting factors W assigned each respective gage, equation (9) becomes

$$I_m = \frac{VB_x\left(W_1 P_1 + W_2 P_2 + W_3 P_3 + \ldots W_n P_n\right)}{n\left(\dfrac{R}{n} + R_m\right)} \tag{10}$$

and

$$E_0 = \frac{VB_x\left(W_1 P_1 + W_2 P_2 + W_n P_n\right)}{n} \tag{11}$$

Equations for Unsymmetrical Orifice Locations

Equations (10) and (11) are applicable where top and bottom airfoil orifices are located at the same chordwise position. However, this location of orifices is not always possible to achieve and an unsymmetrical arrangement must be resorted to. When an unsymmetrical arrangement is used, each orifice requires a separate differential pressure gage, one side of which is connected to a common reference pressure. Since the differential force acting across the airfoil is of interest, the integration of the lower-surface orifices is subtracted from that of the upper surface. Thus, if the same value of reference pressure is used for both lower and upper surfaces, it is canceled out of the equation and its magnitude need not be known. In order to prevent the integrator from having to subtract two large quantities that are close to one another in magnitude, to obtain the final answer, it is desirable to have the reference pressure as close to the average upper-surface or lower-surface pressure as possible. For this reason, absolute pressure gages are not recommended for integrator work.

If an airfoil has orifice locations from 1 to s on the upper surface u and 1 to t on the lower surface l, the equation for output current is given by

$$I_m = \frac{VB_x\left[\overline{W_{1_u}}(P_{1_u} - P_r) + W_{2_u}(P_{2_u} - P_r) + \ldots W_{s_u}(P_{s_u} - P_r)\right]}{(s + t)\left[\frac{R}{(s + t)} + R_m\right]} -$$

$$\frac{VB_x\left[\overline{W_{1_l}}(P_{1_l} - P_r) + W_{2_l}(P_{2_l} - P_r) + \ldots W_{t_z}(P_{t_l} - P_r)\right]}{(s + t)\left[\frac{R}{(s + t)} + R_m\right]} \qquad (12)$$

where P_r is the reference pressure. Since $W_{1_u} + W_{2_u} + \ldots W_{s_u} = W_{1_l} + W_{2_l} + \ldots W_{t_l}$,

$$I_m = \frac{VB_x\left[\overline{W_{1_u}}P_{1_u} + W_{2_u}P_{2_u} + \ldots W_{s_u}P_{s_u} - \left(W_{1_l}P_{1_l} + W_{2_l}P_{2_l} + W_{t_l}P_{t_l}\right)\right]}{(s + t)\left[\frac{R}{(s + t)} + R_m\right]}$$

$$(13)$$

and the equation for output voltage is given by

$$E_0 = \frac{VB_x\left[\left(W_{1_u}P_{1_u} + W_{2_u}P_{2_u} + \ldots W_{s_u}P_{s_u}\right)\right.}{(s + t)} -$$

$$\frac{\left.\left(W_{1_l}P_{1_l} + W_{2_l}P_{2_l} + \ldots W_{t_l}P_{t_l}\right)\right]}{(s + t)} \qquad (14)$$

Equations Relating Integrator Output and Airfoil Coefficients

The normal-force and moment coefficients of an airfoil at spanwise station b_1 are given by the following equations:

$$c_n = \frac{F}{qcb} \tag{15}$$

$$c_m = \frac{M}{qc^2 b} \tag{16}$$

Equations for Force Integrator

Substituting $P_1 = \frac{F_1}{c_1 b}$, $P_2 = \frac{F_2}{c_2 b}$, and so forth, $W_1 = \frac{c_1}{c_x}$, $W_2 = \frac{c_2}{c_x}$, and so forth, $c_1 + c_2 + c_3 + \ldots c_n = c$, and $F_1 + F_2 + F_3 + \ldots F_n = F$ into equation (10), where c_1, c_2, $c_3 \ldots c_n$ is the airfoil-chord section over which each orifice is effective and c_x is the largest of the chord sections, c_1, c_2, c_3, $\ldots c_n$, yields

$$I_m = \frac{VB_x\left(\dfrac{F_1}{c_x b} + \dfrac{F_2}{c_x b} + \dfrac{F_3}{c_x b} + \ldots \dfrac{F_n}{c_x b}\right)}{n\left(\dfrac{R}{n} + R_m\right)}$$

$$= \frac{VB_x F}{c_x bn\left(\dfrac{R}{n} + R_m\right)}$$

however, $c_x = A_1 c$.

Therefore,

$$I_m = \frac{VB_x F}{A_1 cbn\left(\dfrac{R}{n} + R_m\right)} \tag{17}$$

Combining equations (15) and (17) gives

$$I_m = \frac{VB_x q c_n}{A_1 n\left(\dfrac{R}{n} + R_m\right)} \tag{18}$$

or

$$I_m = K_1 q c_n$$

and

$$E_0 = K_2 q c_n \tag{19}$$

where

$$K_1 = \frac{VB_x}{A_1 n\left(\dfrac{R}{n} + R_m\right)}$$

$$K_2 = \frac{VB_x}{A_1 n}$$

Equations for Moment Integrator

A similar analysis of the moment integrator by substituting $P_1 = \dfrac{F_1}{c_1 b}$, $P_2 = \dfrac{F_2}{c_2 b}$, and so forth, $W_1 = \dfrac{a_1 c_1}{(ac)_x}$, $W_2 = \dfrac{a_2 c_2}{(ac)_x}$, and $a_1 F_1 + a_2 F_2 + a_3 F_3 + \ldots a_n F_n = M$ into equation (10), where a_1, a_2, a_3, ... a_n are the moment arms, and $(ac)_x$ is the largest of $a_1 c_1$, $a_2 c_2$, $a_3 c_3$, ... $a_n c_n$ products, yields

$$I_m = \frac{VB_x \left[\dfrac{a_1 F_1}{(ac)_x b} + \dfrac{a_2 F_2}{(ac)_x b} + \dfrac{a_3 F_3}{(ac)_x b} + \ldots \dfrac{a_n F_n}{(ac)_x b}\right]}{n\left(\dfrac{R}{n} + R_m\right)}$$

$$= \frac{VB_x M}{(ac)_x bn\left(\dfrac{R}{n} + R_m\right)}$$

however,

$$(ac)_x = A_2 c^2$$

Therefore,

$$I_m = \frac{VB_x M}{A_2 c^2 bn\left(\frac{R}{n} + R_m\right)} \tag{20}$$

Combining equations (16) and (20) yields

$$I_m = \frac{VB_x q c_m}{A_2 n\left(\frac{R}{n} + R_m\right)} \tag{21}$$

$$I_m = K_3 q c_m \tag{22}$$

and

$$E_0 = K_4 q c_m$$

where

$$K_3 = \frac{VB_x}{A_2 n\left(\frac{R}{n} + R_m\right)}$$

$$K_4 = \frac{VB_x}{A_2 n}$$

In the foregoing analysis, integration has been represented as strictly an addition process. However, in actual practice, such as the use of the moment integrator where negative moments are subtracted from positive ones, units are subtracted as well as added. Proper observance of sign in paralleling bridge outputs is thus necessary for proper integration.

Comparison of Weighting Methods

Shown in appendix C for comparison are results of four weighting methods applied to 16 separate sets of airfoil data. The square-wave

system of weighting has been used in all electrical integrators constructed to date because of its close agreement to the faired method used in the manual integration of data. Here, instead of the fairing normally obtained on manual plots, a line parallel to the airfoil chord is drawn at every orifice point and made to extend half-way to the adjacent orifice on either side of it. The percent of chord associated with the first and last airfoil orifice is measured from a point midway to the adjacent orifice location to the leading and trailing edges, respectively. The weighting factor for each orifice is obtained by dividing its effective chord section by the longest chord section that is assigned to any of the orifice locations. When arrived at in this manner the weighting factor is always 1 or less than 1.

Moment weighting is performed by multiplying the chord assigned to each orifice location by the moment arm as measured from the point at which the moment is desired to the center of the chord section over which the orifice is active. Once this procedure has been carried out for all orifices, division of each product by the largest of the group yields the moment weighting factor. If the constants K_1 and K_2 or K_3 and K_4, as the case may be, are absorbed in meter dial calibration, c_n and c_m may be obtained by dividing the integrator output readings by the dynamic pressure q.

DESCRIPTION OF EQUIPMENT AND EXPERIMENTAL TESTS

In September 1948 the need for a more rapid means of reducing lift and pitching-moment data from a series of proposed Langley 16-foot-high-speed-tunnel propeller tests became acute. As a solution to this problem, the model A pressure integrator came into being. Aside from the normal considerations of pressure measurement on airfoils, the problem was further complicated by the necessity of using a pressure-transfer device and the correction necessitated by the acceleration effect on the air confined in the pressure tubes on the rotating propeller. Model A was therefore constructed and consisted of both force and moment integrators.

Model A Integrator

In this unit, 24 chordwise pressure orifices (12 on each side of the propeller blade) were connected to a similar number of identical ±10-pound-per-square-inch electrical differential pressure gages of the unbonded wire strain-gage type located in each of the force and moment units. A gage for each orifice was necessitated by nonsymmetrical orifice location on the upper and lower surfaces of the model. The pressures

measured by the gages were also read on a liquid multitube manometer board. One side of all gages was referenced to the tunnel test chamber as was also the manometer sump. Because of the location of the orifices, each pressure was effective over a different physical area on the propeller surface. Weighting was accomplished as previously described in the sections entitled "Introduction" and "Theory." Thus, the normal force F was obtained by the use of equation (12). As shown in the section entitled "Theory," in order to obtain this differential force acting on the propeller blade, it is necessary to integrate the force acting over the cambered-surface orifices 1 to 12, and subtract from this quantity the integrated force acting on the thrust-surface orifices 13 to 24. This procedure was carried out in the force integrator by proper observation of sign in paralleling gage outputs.

For orientation and to show the relative simplicity of construction, an internal view of the force integrator is shown in figure 9. In order to minimize gage errors due to temperature variation, the integrator was placed in a thermally insulated box which was temperature-regulated at approximately 110° F. The integrator output was indicated on a Weston type 622 50-0-50 microammeter for moment and 0-100 microammeter for force. A dummy 400-ohm bridge (see circuit diagram of fig. 10) was added to permit zero output-current adjustment and thus compensate for the small zero unbalance in the gages. The moment integrator is physically the same as the force unit, only the weighting factor and the quantities added and subtracted being changed. Since the moment integrator was designed to read the resultant moment about the quarter-chord point, it possesses 23 instead of 24 pressure gages because orifice 16 occurs at the quarter-chord point. Calibration was accomplished by placing pressure P_1 on gages 1 to 12 and pressure P_2 on gages 13 to 24, with $P_2 > P_1$. Areas under the force and moment curves were easily calculated and plotted on the ordinate with the corresponding meter readings plotted on the abscissa. Calibration curves for the two integrators are shown in figure 11. Here the integrated areas under the force and moment curves are plotted against meter readings and are observed to be straight lines.

Experimental tests.- Tunnel tests have been made with this unit and results plotted in figure 12, along with those from manual integration, for comparison purposes. In order to obtain these data, a test propeller with 12 orifices on the cambered surface and 12 on the thrust surface was connected through a pressure-transfer device to a liquid manometer and also tied into the force and moment integrators. The results from the electrical integrators were converted to normal-force coefficient c_n and moment coefficient c_m. Thus,

$$c_n = \frac{Fk_5}{cqx}$$

$$c_m = \frac{Mk_5}{c^2 qx}$$

where k_5 is the tunnel correction factor, dependent upon temperature and propeller rotational speed and qx is the velocity pressure across the x-station of the propeller. Conversion was performed by multiplying the force-integrator output F/c and moment-integrator output M/c^2 by k_5 and dividing by qx. These coefficients were then plotted against the propeller advance-diameter ratio J, a parameter relating tunnel speed, propeller rotational speed, and propeller diameter, where

$$J = \frac{V}{ND}$$

The liquid manometer records were in turn read, plotted as pressure-distribution diagrams similar to figure 1, and integrated with a planimeter. These results were also plotted in figure 12.

Discussion of results.- The plots of force and moment coefficients against J, as seen in figure 12, indicate scatter from the best faired line which is about the same for both the electrical integrator and manual integration from liquid-manometer data. In order to see the errors that would be introduced in individual reading, plotting, and fairing techniques, the manual data were plotted and faired by two people and the results compared. Differences between the two manual integrations were found to be of the same order of magnitude as those between data from manual and electrical integration. Although not shown in the curves of figure 12, some cases existed where deflection of the electrical meter was only 1 or 2 percent of its full-scale deflection and appreciable discrepancy was found between electrical and manual systems. More sensitive meters and range switches would minimize this discrepancy. The promising results obtained from these simple integrators established them as prototypes and led to the design of a model B integrator.

Model B Integrator

The model B integrator unit, similar to the model A, contains two electrical integrators, one for normal force and one for pitching moment about the quarter-chord point of the airfoil. As in the A unit, the only difference between the normal-force and moment integrators is in the numerical value of the weighting factors. All gages are temperature-regulated as before. Physically, both normal-force and moment integrators have been built into the same chassis; therefore, they are discussed as one unit. Figures 13 and 14 are photographs of the composite instrument which consists of three basic components - the sensing and integrating circuit, the measuring circuit, and the computing circuit.

This combination thus permits an integration of force and moment, followed by a subsequent computation of coefficients c_n and c_m, and plotting of these coefficients against Mach number on graph paper. As seen by referring to figure 14, tunnel q and Mach number are set into the computer manually.

Orifice locations on the upper and lower airfoil surfaces were located at the same percent-chord positions, one differential pressure gage per pair of orifices and equation (11) could therefore be used. The force integrator thus contains twenty-two ±10-pound-per-square-inch electrical differential pressure gages; the moment integrator contains twenty-one, properly weighted with precision resistors. Their outputs are connected in parallel so as to give a quantity proportional to qc_n and qc_m (equations (19) and (22)). The integrator supply voltage is maintained constant by sampling and adjusting from time to time its relation to a standard cell voltage, and thus creates a null point which is read on a panel type of galvanometer which, along with associated adjusting knobs, is visible in figure 14.

The computing circuit obtains coefficients c_n and c_m by dividing the integrator outputs by q. This division is obtained by use of a bucking bridge circuit where the output of the integrator is matched in a null system by the output voltage of the computing bridge. The unbalanced voltage is detected by a servo amplifier which is part of the servo loop for positioning a multiple-turn helical slide-wire in the computing bridge. The sliding contact is in turn mechanically coupled to a pointer and print carriage. The movements of the pointers were made proportional to coefficients c_n and c_m by setting the voltage of the computing bridges directly proportional to q. This voltage is adjusted by means of a 10-turn helical potentiometer, the movement of which is calibrated in terms of pounds per square foot, and is set by a dial on the front panel of the instrument.

The print mechanism is operated by a lever switch on the front panel, which permits a plot to be made on both charts at any desired point as described previously. The position of the printer along the horizontal scale determines the values of c_n and c_m. The chart paper is driven past this horizontal scale by a Selsyn receiver which in turn is driven by a Selsyn transmitter located in the front panel. The transmitter has its rotation calibrated in Mach number. Thus, the desired output from the instrument, a plot of c_n and c_m against Mach number, is obtained while the tunnel is in operation.

Calibration of the instrument was made by applying the same differential pressure to all the gages of the integrators. Effectively, this calibration produces a rectangular pressure distribution of known area.

With the q setting at a value corresponding to the highest Mach number (M = 1.0) the full scale of the coefficient dials were set. Checks were made by varying the applied differential pressure and the q network. As a further check of weighting, various pressure patterns were applied to the gages with q constant. Table I gives a comparison of values obtained from the electrical integrator by using a precision manometer to set the pressures with those calculated from the pressure used. The magnitudes of the average errors are 0.0033 in normal-force coefficient and 0.00072 in moment coefficient. These errors compare very favorably with average coefficient errors of 0.0075 in normal force, and 0.002 in moment, considered satisfactory by tunnel personnel. These desired limits represent errors of 1 percent or less of full-scale-range values of 2.0 for the normal-force coefficient and 0.4 for the moment coefficient, for which the equipment was designed.

Experimental tests.- Model B integrator was tested in the following manner:

1. The electrical integrator was balanced at the lowest value of q for highest accuracy of balancing.

2. Since the points were taken in Mach number steps starting with Mach number 1.0 and progressing to the lower values, the q and Mach number dials of the integrator were set for Mach number 1.0 before the tunnel was run.

3. The tunnel was then started. A signal from the tunnel operator at each point indicated that the proper velocity had been reached. When the integrator operator saw that the pressures had stabilized, he signalled the tunnel operator so that a manometer-board picture could be taken at the same time a point was being plotted on the integrator.

It was impossible for the tunnel operator to hold the tunnel accurately at the Mach number preset on the integrator; therefore, a difference existed between the true q of the tunnel and the set q of the integrator. In order to compensate for this difference a correction was applied to the data in integrating the results.

Table II contains tabulated data showing the correlation between electrical integrator plots and data obtained from integrating faired manometer film data from tunnel tests. Figures 15 and 16 are actual integrator plots of c_n and c_m against Mach number. For comparison purposes, the manometer film data have also been plotted in this graph. As can be determined from table II, the average magnitudes of the differences between the electrical integrator and the manometer film, read and integrated on the basis of a faired curve, are 0.0083 in normal-force coefficient and 0.0015 in moment coefficient.

Discussion of results.- The calibration errors noted previously represent actual instrument errors since this calibration compares integrator output with the actual value calculated in a square-wave manner, which is the same as the method used by the electrical integrator. Tunnel tests, however, compare integrator output with that obtained by manually integrating a faired curve with a planimeter and represent, in addition to instrument error, differences between the square-wave method and fairing method of representing area, as shown in appendix C. As noted in appendix C, various methods of determining coefficients manually from the same pressure data result in slightly different answers. Thus, a completely rigorous analysis of instrument error, when applied to tunnel work, is impossible for want of an exact standard for comparison. However, a comparison of a faired curve to the tunnel standard indicates that the electrical integrator produces satisfactory data.

Since the outputs of the force and moment integrators are subsequently divided electrically within the apparatus to render plots of c_n and c_m against Mach number, a fixed error in the force-integrator measurement would manifest itself as a decreasing error in c_n with an increase of Mach number. This reduction in error is true even if the absolute value of c_n does not change since both numerator and denominator of the coefficient equation $c_n = \dfrac{F/cb}{q}$ are increasing in value. This trend can be seen by referring to the Mach number points 0.295 and 0.84 for the data of table II. Here the c_n error decreases in magnitude from 0.02 to 0.007 as the Mach number varies between 0.295 and 0.84 even though the magnitude of the error in pounds is greater at the higher Mach numbers.

Model C Integrator

The model C integrating unit was constructed to expand the capacity and increase the accuracy of the previous model. Model C consists of eight normal-force and eight moment channels of integrators, a null type of self-balancing servo unit for each channel with built-in indicators and two 8-channel printers for recording information. The integrator units, as in model B, sample 22 differential pressures across the airfoil, and have an output of qc_n and qc_m, the qc_m being about the quarter-chord point. As before, the pressure gages are mounted in a temperature-controlled box. This unit is in turn rack and panel mounted as shown in figure 17. The coefficient-computing circuit of model B is eliminated here and the integrator output voltage is converted into an indicated answer on direct-reading revolution counters and a shaft rotation for the operation of printers by a self-balancing servo incorporating a 25-turn helical measuring potentiometer. With this system,

integrator errors account for 90 percent of the total error. Sixteen channels of printer are Selsyn-coupled to the balance units to provide simultaneous printing and indicating of the values qc_n and qc_m. Coefficients can then be quickly obtained in integrating the data by dividing by q. Balancing, indicating, and printing units are shown in figure 18. All force channels are designed for the range in qc_n of -441 to 1225 pounds per square foot. All moment channels have the range in qc_m of -165 to 165 pounds per square foot.

Calibration checks of this unit have resulted in the average error for all channels of 1.21 pounds per square foot in qc_n and 0.25 pounds per square foot in qc_m. For comparison with calibration checks on the model B integrator, conversion can be made to coefficient form for a low and high value of q of 200 and 800 pounds per square foot, between which most of tunnel tests will fall. For a q of 200 pounds per square foot the error in c_n is 0.0061 and that in c_m is 0.0013. When q is 800 pounds per square foot the errors reduce to 0.0015 in c_n and 0.00031 in c_m. These errors compare very favorably with the before-mentioned acceptable errors of 0.0075 in c_n and 0.002 in c_m.

Model D

Model D was constructed with the use of the NACA miniature electrical pressure gage as the pressure sensing unit for the measurement of both static- and dynamic-force coefficient. This unit consists of a 12-differential-pressure-gage integrator, a modified ring demodulator, a balance circuit, a self-balancing potentiometer for static measurements, and a deflection-coil galvanometer for dynamic use. The designed full-scale value of qc_n was 2160 pounds per square foot. Laboratory checks of this unit have resulted in an average error of 13.9 pounds per square foot in qc_n.

Since this unit was designed principally to measure dynamic quantities, required accuracies were relaxed from the more rigid ones of the previous models. In this unit, errors of 50 pounds per square foot in the quantity qc_n are considered acceptable. The results of the dynamic testing have not been checked to date for want of a standard for comparison.

Models E and F

In addition to the foregoing models a telemetering model E has been constructed and successfully used in rockets, and at present a model F is being constructed for flight use.

ADDITIONAL CONSIDERATIONS IN DESIGN OF PRACTICAL INTEGRATORS

Weighting Procedure

While exact values of resistors to be inserted in the individual integrator gage circuits can be calculated if weighting factor and gage sensitivity are known, experimental determination of these resistance values is more desirable. By this procedure no errors due to unequal bridge resistances will result. This adjustment can easily be made in the following manner. Connect the output of all integrator gages plus the zero balancing bridge in parallel and run this output to the indicator unit in the same manner as they will exist in the finished integrator. Now energize each gage in turn from the integrator voltage source through two decade resistance boxes, one located in each of the two gage voltage leads. Care must be exercised to insure that the resistance values set on both decade boxes are always the same. The process starts with the most insensitive gage of the group, that is, the gage with the constant of proportionality B_x. This reference gage is then associated with the orifice possessing the largest weighting factor and full-supply voltage applied by setting the decade resistance values at zero. After balancing the integrator for zero output at zero pressure, full-scale pressure is applied to the reference gage and the output noted. The decade boxes are then moved to the next gage; the unit zeroed at no pressure, then the previously determined full-scale pressure is applied. The decade boxes are then adjusted until the output current bears the same relationship to that of the reference gage as do their weighting factors. Since varying the decade-box resistance may have an effect on system zero balance, the process must be repeated until the zero shift is negligible. All succeeding gages are treated in a similar manner.

In order to eliminate interaction between bridges during experimental adjustments, the weighting resistors must be placed in the voltage input. Although weighting can be accomplished by placing resistors in the gage output circuit, this procedure introduces interaction due to the changing load and precludes experimental adjustment of weighting. As shown in appendix A, the gage load resistance does not change with resistance in the voltage leads.

In the model B integrator, flexibility of weighting was achieved by placing all gage voltage-dropping resistors in a plug-in unit. In this manner, airfoils possessing different orifice locations were quickly accommodated by plugging in the resistor box containing the appropriate weighting.

Whenever possible, airfoil orifice locations should be chosen for uniform spacing. This spacing results in a minimum variation of

weighting factors, which in turn permits large integrator outputs. As seen in equations (10) and (11), maximum integrator output occurs when all weighting factors are equal. Under these conditions full-rated voltage can be placed on all gages. It is also noted by referring to equation (11) that the maximum no-load voltage output of the integrator, when all its bridges are energized by the same forcing function, cannot exceed the no-load output voltage of one of the bridges alone when subjected to the same forcing function. The current output, however, can be increased considerably by decreasing circuit resistance with the proper choice of indicator units.

Factors Affecting Accuracy

Accuracy in the integrated results is dependent upon the following factors:

Type of sensing unit.- With the use of wire strain-gage sensing units, ambient temperature and vibration effects were eliminated by placing gages in a temperature-regulated box and by shock mounting. When these precautions have been taken, gage nonlinearity, hysteresis, creep, and zero drift remain as factors determining sensing-unit accuracy. Tests have been conducted with twenty-two ±15-pound-per-square-inch sensing units in parallel to simulate integrator operation, and the following errors have been observed.

Maximum hysteresis and creep, percent of greatest pressure applied   0.4
Average nonlinearity, percent 0.05
Average zero drift, percent per hour of gage full scale 0.05

No attempt was made to separate hysteresis from creep. Nonlinearity has been expressed by dividing the average deviation from a mean straight line by the full-scale pressure and converting to percent. From the foregoing check the gage hysteresis is obviously the limiting factor in sensing-unit accuracy. The inductance pressure gage used in model D displayed better hysteresis characteristics than the wire strain-gage unit but at the same time introduced balancing problems singular to alternating-current bridges.

Weighting.- Over-all integrator accuracy is also dependent upon the care with which each gage is weighted. Errors in setting the gage voltage values and instability in these units contribute directly to the final error.

Bridge voltage control.- If a deflection-measuring system is used, the error is increased by poor regulation of the integrator supply voltage in a direct manner, similar to that of weighting. A null system can be made independent of moderate supply-voltage fluctuations and is thus preferred.

Indicator or recording.- Whichever indicator or recording system is used, the inherent accuracy should be greater than that realizable from the integrator alone. For static conditions, this goal is easily realized with a servo-operated, self-balancing null system. In dynamic measurements this goal is not easily attained. As a result, the total error is increased.

Stability of resistors.- The values of all integrator resistors are critical and, once determined, should not change. In order to prevent aging and sensitivity to the small temperature changes present, all resistors used in the integrators discussed in this paper were constructed with low-temperature-coefficient wire.

Potentiometers.- Bridge balancing and measuring potentiometers are used. The balancing potentiometer must possess resolution for fineness of balance and stability once balance has been achieved. Repeatability and linearity are of secondary importance; however, in circuits where a measuring potentiometer is used to obtain the final answer, linearity, repeatability, resolution, and stability are of prime importance. A popular combination is the 10-turn helical potentiometer for balancing and a 25-turn helical potentiometer for measuring.

Number of points sampled.- Discrepancies among alternate methods of integrator weighting, square wave, parabolic, and so forth, decrease as the number of points where pressure is sampled is increased. It is thus desirable to have the maximum number of sampling points.

Shape of curve.- Final accuracy is dependent upon the pressure distribution experienced over the airfoil. If the pressure diagram has large gradients and sharp breaks, the integrator weighting less closely fits the curve and greater error results.

Reliability

Time spent in maintenance of these integrators has been small. Since the model B integrator has had the longest period of continuous service, the maintenance performed on it is briefly outlined. During the construction and initial calibration phase it was necessary to replace one pressure gage because of an intermittant open circuit within the gage itself, repair the output connection to a second gage, adjust the printer, and replace the helical potentiometer in the integrator voltage circuit because of roughness of the potentiometer interfering with the fine setting of voltage. Subsequent to these adjustments, in over a year of tunnel operation the equipment has been check-calibrated three times with no change of calibration detected and maintenance has consisted of periodic changing of batteries.

CONCLUDING REMARKS

The electrical integrators described herein are practical, continuously useful, nonexperimental research tools of appreciable significance to the aerodynamisist because of their great appeal as time and labor savers. These units reduced manual-integration time by a factor of 6 to 10 when subsequent corrections were added to the answer, and as high as 30 when the answer was presented in its final form.

In addition to saving a large amount of computing labor wherever used, the electrical integrator gives the same accuracy in the final plot as manual methods of obtaining force data from pressure surveys. Variations between the electrical integrator and manometer film data are no greater than those experienced in successive readings and planimeter integration of the same film.

One characteristic of all integrators, irrespective of the method of weighting employed, is their consistency of weighting each set of data in a similar manner. This characteristic has the advantage that integrated answers are not dependent upon the technique of the manual plotter. In eliminating computing labor, the electrical integrator also eliminates a large number of man-made computing mistakes.

Much discussion has centered around the possibility of adverse effects that steep slopes in the pressure-distribution diagrams would have on the accuracy of the square-wave method of fairing. All the tunnel-data checks have shown negligible errors from this source.

Model E designed for use on rockets permitted a pressure determination of force and moment coefficients c_n and c_m in flight, heretofore unattainable because of limitation of available telemetering channels.

Compared to other integrators the electrical integrator is considerably more flexible and is constructed of commerically available parts. The principal disadvantages are the high initial cost and increased complexity.

Langley Aeronautical Laboratory
      National Advisory Committee for Aeronautics
            Langley Field, Va., October 8, 1951

APPENDIX A

EQUIVALENT BRIDGE IMPEDANCE WHEN DROPPING RESISTORS ARE USED

The equivalent Thévenins series impedance Z_1, shown in figure 6, of a Wheatstone bridge composed of equal resistance arms R with a voltage-dropping resistor in the power-supply leads is given by the following equation:

$$Z_1 = \frac{\left(R + \dfrac{RR_d}{R_d + 2R}\right)^2}{2\left(R + \dfrac{R_d}{R_d + 2R}\right)} + \frac{R^2}{R_d + 2R}$$

$$= \frac{R}{2} + \frac{RR_d}{2\left(R_d + 2R\right)} + \frac{R^2}{R_d + 2R}$$

$$= R\left[\frac{1}{2} + \frac{R_d}{2\left(R_d + 2R\right)} + \frac{R}{R_d + 2R}\right]$$

$$= R$$

APPENDIX B

TOTAL METER CURRENT OF TWO WHEATSTONE BRIDGES IN PARALLEL

Figure 4 gives the equivalent circuit of two paralleled Wheatstone bridges. Solution of this circuit for total meter current I_2 is easily accomplished by using the principle of superposition. With only bridge 1 active, as shown in figure 7, the current contributed by this bridge alone can be evaluated in the following manner:

Given:

$$E_1 = \frac{V \, \Delta R_1 X_1}{R}$$

$$E_2 = 0$$

where

$$X_1 = \frac{R}{R + R_{d_1}}$$

Writing the equation for the outside loop gives

$$\frac{V \, \Delta R_1 X_1}{R} = I_1'R + I_2'R_m$$

and the equation for the right-hand loop is

$$0 = I_2'R - I_1'R + I_2'R_m$$

Combining the two loop equations yields

$$I_1'R = I_2'\left(R + R_m\right)$$

$$I_1' = \frac{I_2'\left(R + R_m\right)}{R}$$

Substituting this value of I_1' into the outside-loop equation yields

$$\frac{V\ \Delta R_1 X_1}{R} = I_2'R + 2I_2'R_m$$

$$I_2' = \frac{V\ \Delta R_1 X_1}{2R\left(\frac{R}{2} + R_m\right)}$$

In a similar manner, analysis of the circuit of figure 8 determines the value of output current contributed by bridge 2 as follows:

Here

$$E_1 = 0$$

$$E_2 = \frac{V\ \Delta R_2 X_2}{R}$$

where

$$X_2 = \frac{R}{R + R_{d_2}}$$

Writing the equation for the right-hand loop gives

$$E_2 = \left(I_2'' - I_1''\right)R + I_2''R_m$$

and the equation for the outside loop is

$$0 = I_1''R + I_2''R_m$$

Combining the two loop equations yields

$$I_1" = \frac{-I_2"R_m}{R}$$

Substituting this value of $I_1"$ into the right-hand loop equation yields

$$E_2 = I_2"\left(R + 2R_m\right)$$

$$I_2" = \frac{V \, \Delta R_2 X_2}{2R\left(\frac{R}{2} + R_m\right)}$$

Total meter current is thus given as

$$I_2 = I_2' + I_2"$$

$$= \frac{V\left(X_1 \, \Delta R_1 + X_2 \, \Delta R_2\right)}{2R\left(\frac{R}{2} + R_m\right)}$$

APPENDIX C

COMPARISON OF WEIGHTING METHODS

A comparison is made of faired, parabolic, square-wave, and mixed-weighting-factor methods of obtaining force and moment coefficients from 16 tunnel tests ranging in pressure-distribution patterns from those having large pressure differentials ahead of the quarter-chord point to those with high differential pressures behind this point. Faired data were obtained by plotting the pressures as a pressure-distribution diagram and integrating with a planimeter. All others consisted of multiplying each pressure with a predetermined weighting factor, dependent upon the method used, and summing the products. The mixed weighting factor was determined by applying parabolic weighting from 0 to 10 and from 90 to 100 percent chord and square-wave weighting from 10 to 90 percent chord.

The coefficients of the various weighting methods are presented in the following table:

Diagram	Faired		Square wave		Parabolic		Mixed	
	c_n	c_m	c_n	c_m	c_n	c_m	c_n	c_m
1	0.637	0.0121	0.647	0.0135	0.624	0.0088	0.633	0.0102
2	.673	.0166	.677	.0180	.653	.0128	.660	.0144
3	.666	.0182	.667	.0184	.644	.0137	.651	.0152
4	.716	.0258	.713	.0270	.693	.0230	.699	.0241
5	.754	.0331	.753	.0330	.726	.0288	.739	.0300
6	.8146	.0306	.828	.0330	.811	.0304	.815	.0305
7	.701	-.0213	.714	-.0189	.699	-.0203	.702	-.0195
8	.653	-.0267	.660	-.0276	.660	-.0283	.649	-.0275
9	.593	-.0287	.603	-.0298	.591	-.0299	.593	-.0292
10	.536	-.0270	.547	-.0281	.535	-.0279	.537	-.0272
11	.475	-.0193	.489	-.0196	.476	-.0189	.478	-.0182
12	.363	.0318	.368	.0344	.359	.0326	.361	.0331
13	.374	.2972	.378	.0320	.371	.0295	.373	.0300
14	.436	.0049	.441	.0055	.433	.0041	.435	.0044
15	.513	-.0329	.513	-.0330	.511	-.0333	.513	-.0330
16	.572	-.0597	.562	-.0585	.564	-.0582	.565	-.0584

With the faired data as a standard, the following table gives the average deviation, based on the 16 tunnel tests, of the square-wave, parabolic, and mixed methods from this standard:

Coefficients	Square wave	Parabolic	Mixed
c_n	0.0071	0.0087	0.0053
c_m	.0012	.0017	.0013

The mixed weighting factor gives the closest agreement for force while the square-wave method results in the best moment answer.

TABLE I

COMPARISON OF CALCULATED DATA WITH DATA OBTAINED FROM MODEL B

ELECTRICAL INTEGRATOR BY APPLYING PRESSURES

WITH THE USE OF PRECISION MANOMETERS

Mach number	qc_n Electrical (lb/sq in.)	qc_n Calculated (lb/sq in.)	Error (lb/sq in.)	c_n Electrical	c_n Calculated	Error	qc_m Electrical (lb/sq in.)	qc_m Calculated (lb/sq in.)	Error (lb/sq in.)	c_m Electrical	c_m Calculated	Error
0.3	0.684	0.685	0.001	0.7852	0.786	0.0008	-0.0171	-0.01682	0.00028	-0.0196	-0.0193	0.0003
.5	1.522	1.517	-.005	.7003	.698	-.0023	.03042	.0276	-.00282	.0140	.0127	.0013
.811	3.337	3.309	-.028	.7585	.752	-.0065	-.1408	-.1452	-.0044	-.032	-.033	-.001
.90	3.861	3.841	-.02	.782	.778	-.004	-.2691	-.2716	-.0025	-.0545	-.055	-.0005
1.00	3.357	3.343	-.014	.6167	.614	-.0027	-.4274	-.4301	-.0027	-.0785	-.079	-.0005

NACA

TABLE II

COMPARISON OF MODEL B ELECTRICAL INTEGRATOR DATA WITH THAT OBTAINED

FROM INTEGRATING A FAIRED PRESSURE-DISTRIBUTION CURVE

Mach number	qc_n Electrical (lb/sq in.)	qc_n Manual (lb/sq in.)	Difference (lb/sq in.)	c_n Electrical	c_n Manual	Difference	qc_m Electrical (lb/sq in.)	qc_m Manual (lb/sq in.)	Difference (lb.sq in.)	c_m Electrical	c_m Manual	Difference
0.295	0.5705	0.587	0.0165	0.655	0.675	0.02	0.0117	0.0127	0.001	0.0135	0.015	0.0015
.395	.967	.978	.0103	.655	.661	.006	.0237	.0215	.0014	.016	.017	.001
.495	1.467	1.469	.002	.675	.676	.001	.0424	.0428	.0004	.0195	.020	.0005
.599	2.066	2.068	.002	.710	.711	.001	.06578	.0696	.0038	.023	.024	.001
.694	2.932	2.903	-.029	.805	.797	-.008	.09833	.1045	.0062	.027	.029	.002
.795	3.397	3.330	-.067	.785	.770	-.015	-.0995	-.0856	.0139	-.023	-.020	.003
.840	3.343	3.310	-.033	.720	.713	-.007	-.1694	-.165	.0044	-.0365	-.035	.0015

NACA
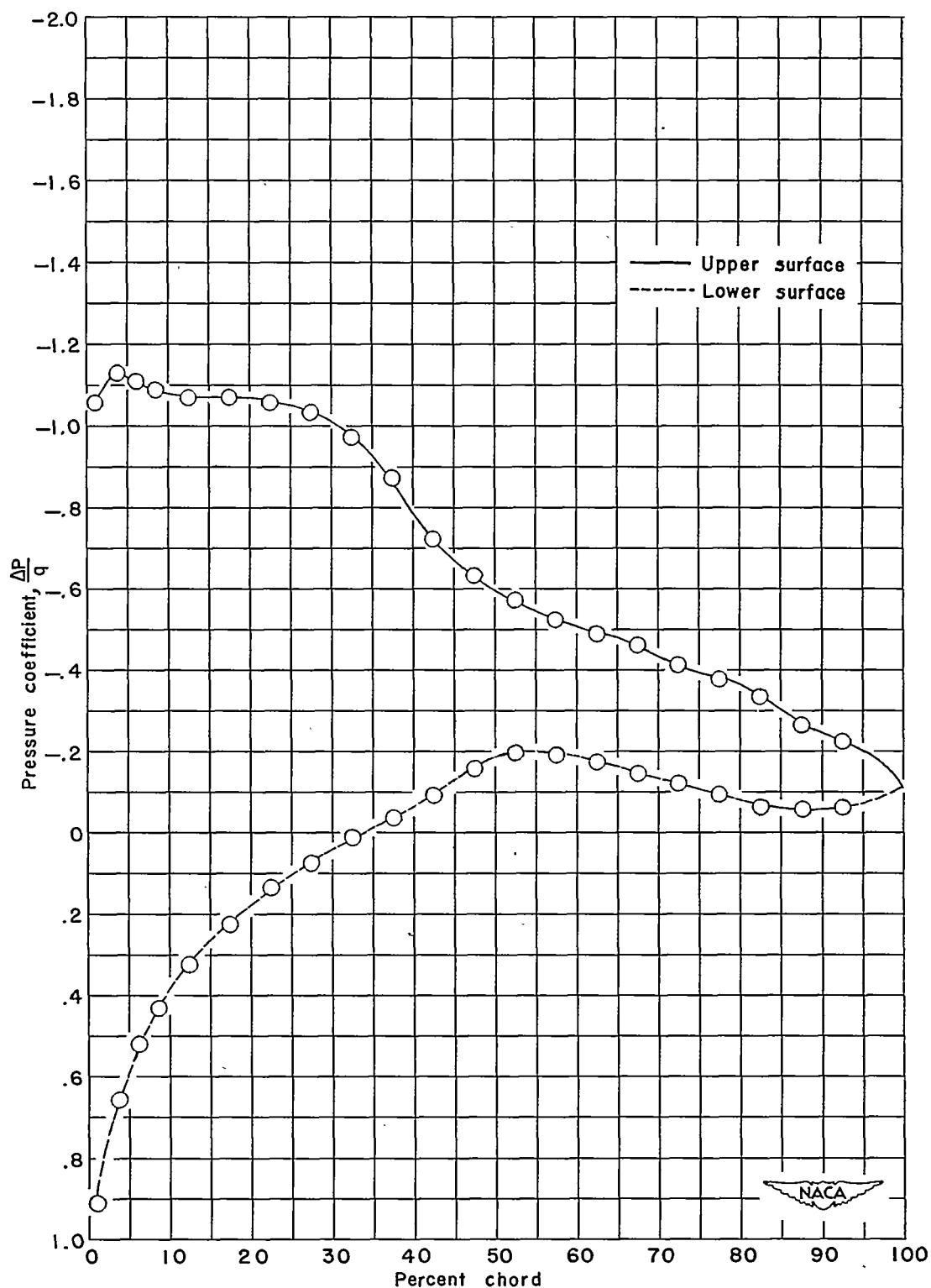
Figure 1.- Typical pressure-distribution diagram.
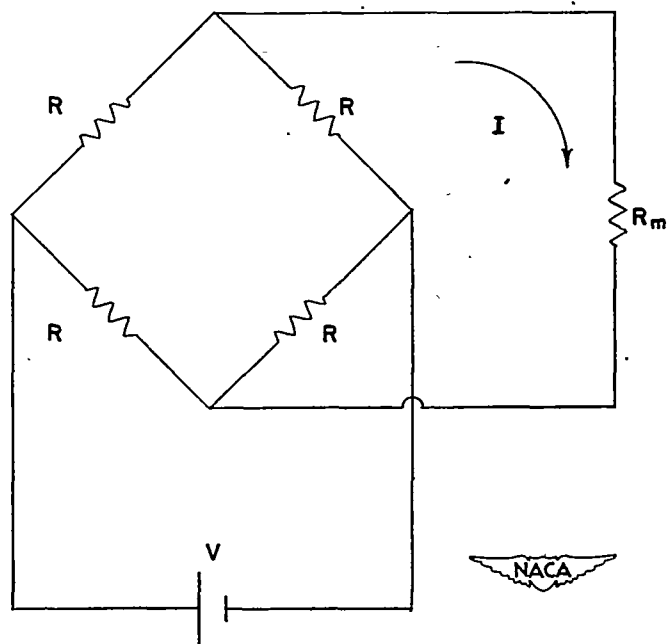
Figure 2.- Wheatstone bridge.
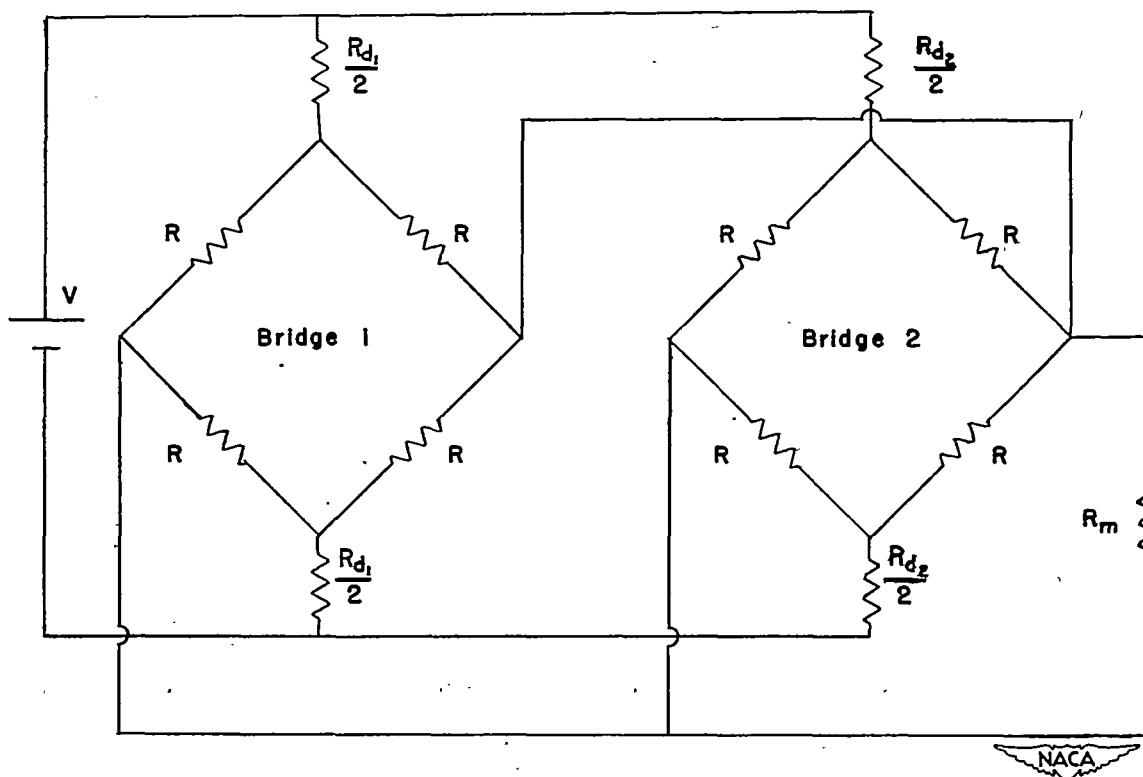
Figure 3.- Two paralleled Wheatstone bridges.
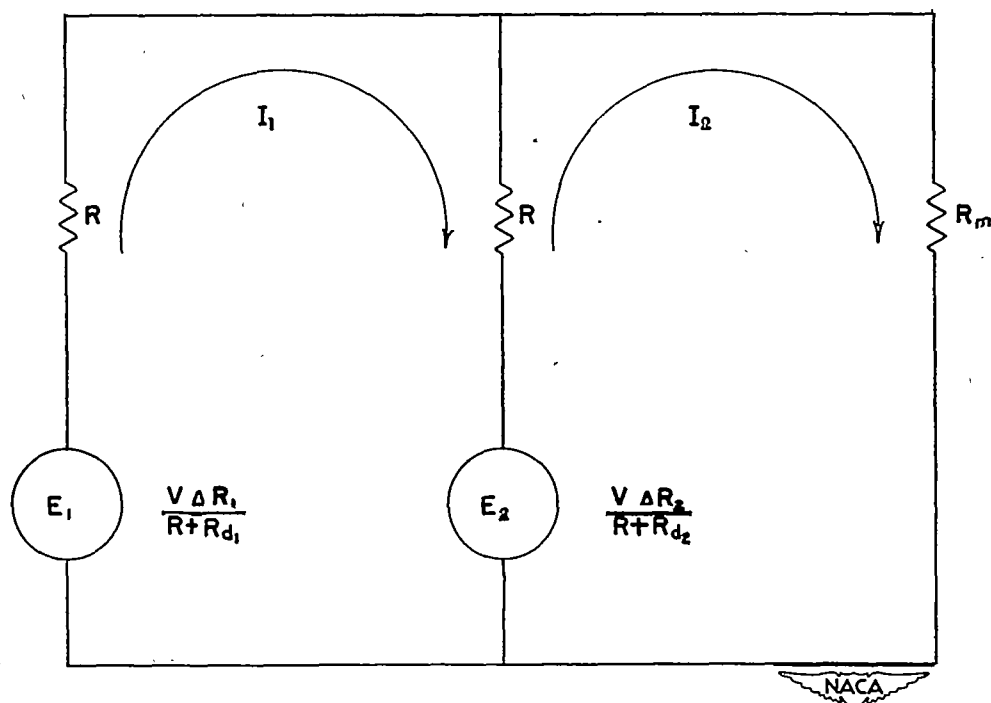
Figure 4.- Equivalent circuit of figure 3.
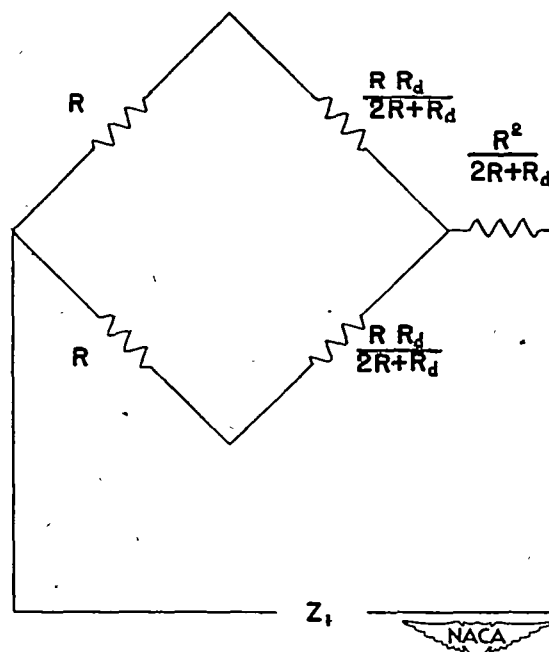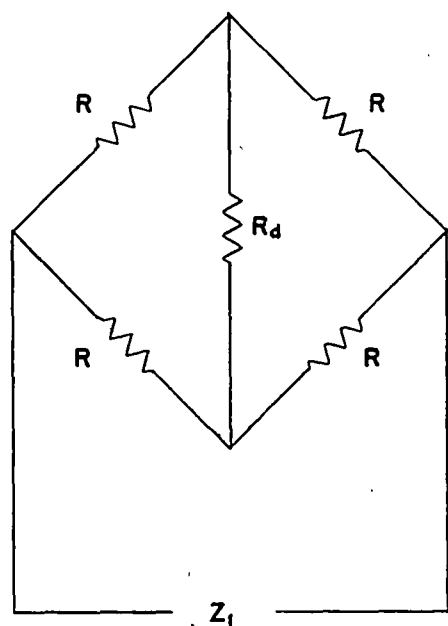
Figure 5.- Thévenins series resistance.

Figure 6.- Y equivalent of figure 5.
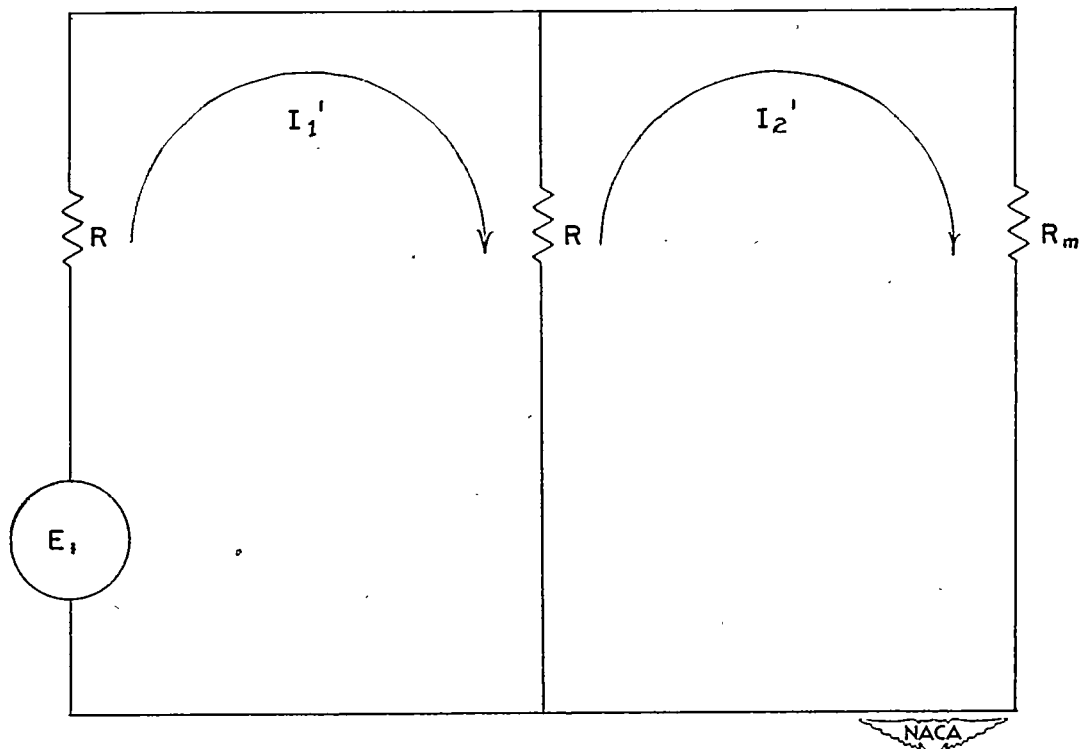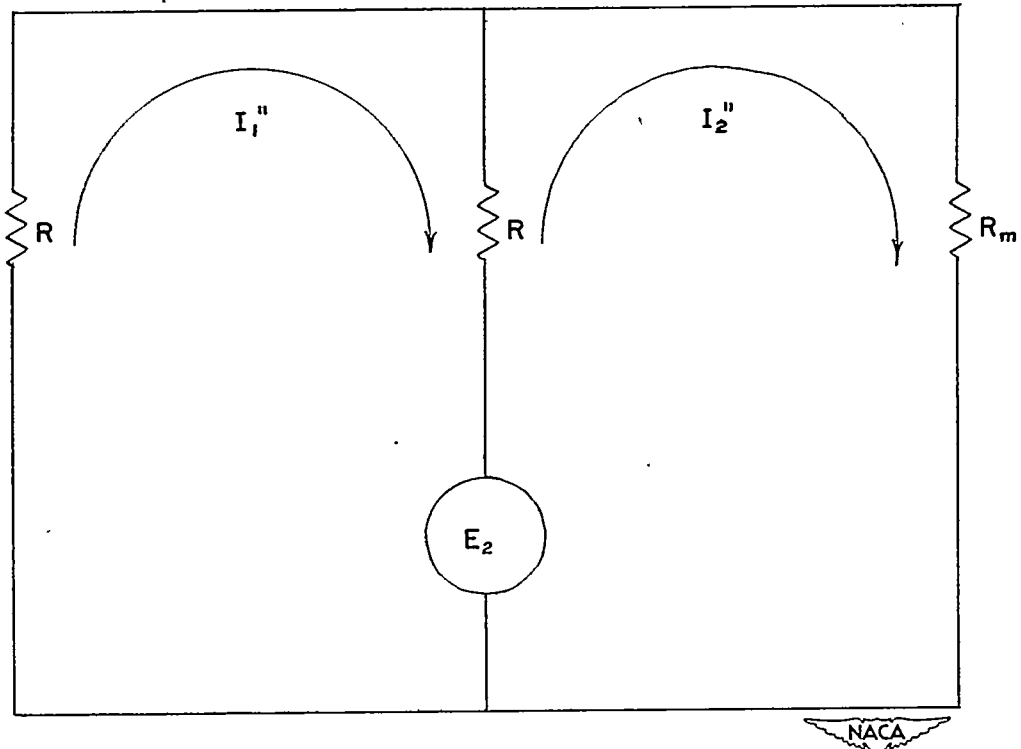
Figure 7.- Circuit of figure 3 with only generator 1 active.

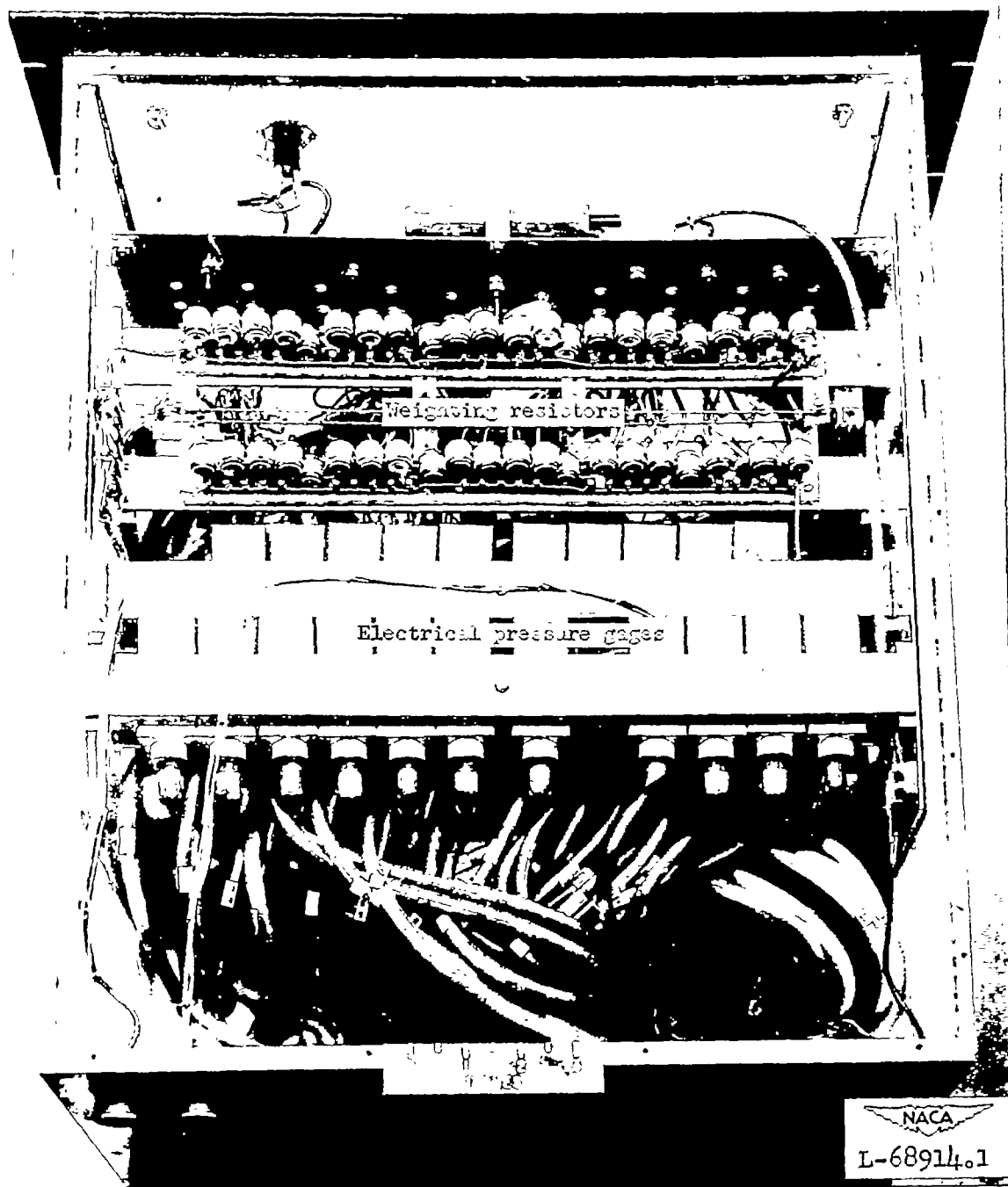Figure 8.- Circuit of figure 3 with only generator 2 active.
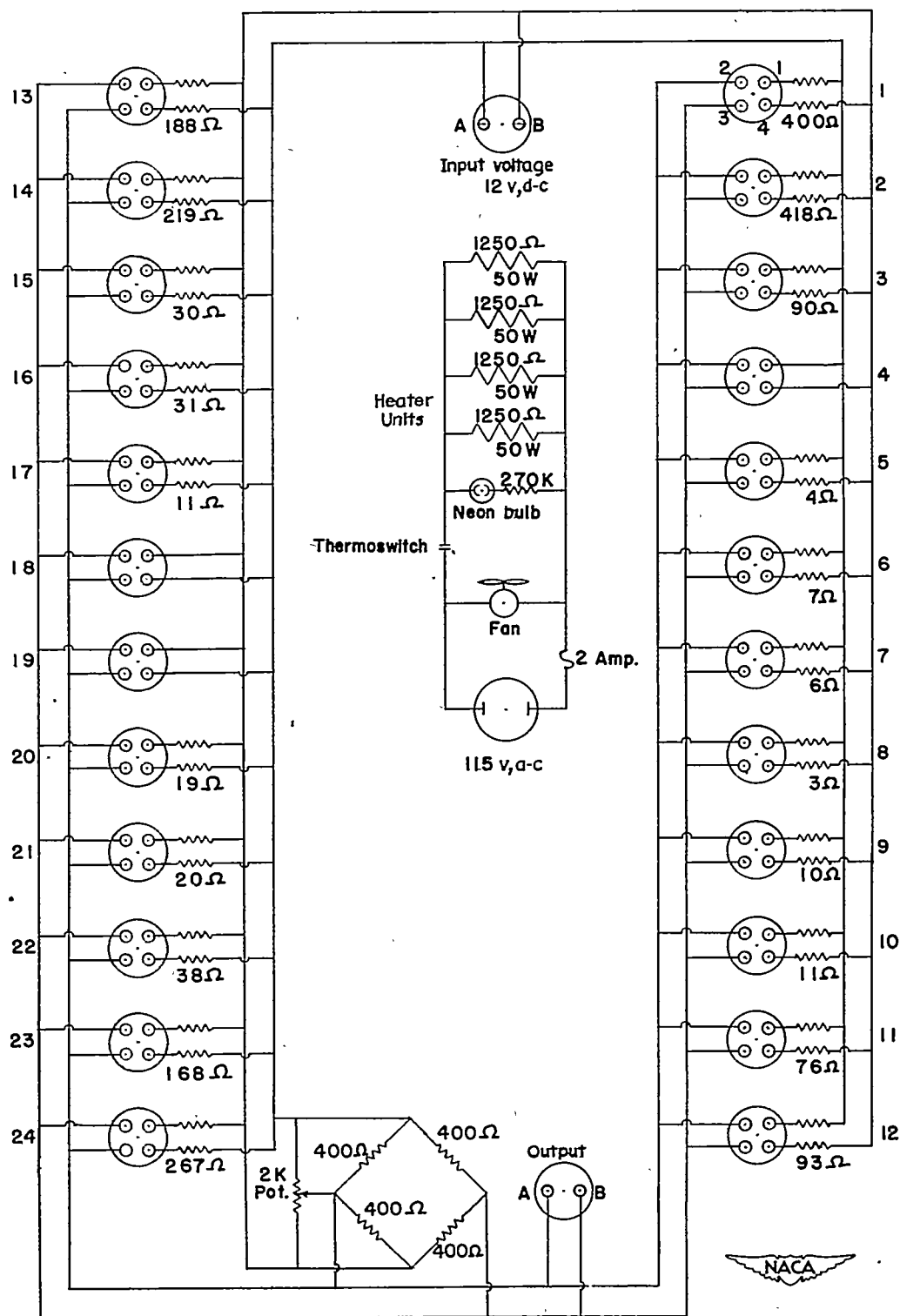
Figure 9.- Force-integrator network.

Figure 10.- Circuit diagram of model A force integrator. Bridge voltage dropping resistors are used in matched pairs of the value shown.
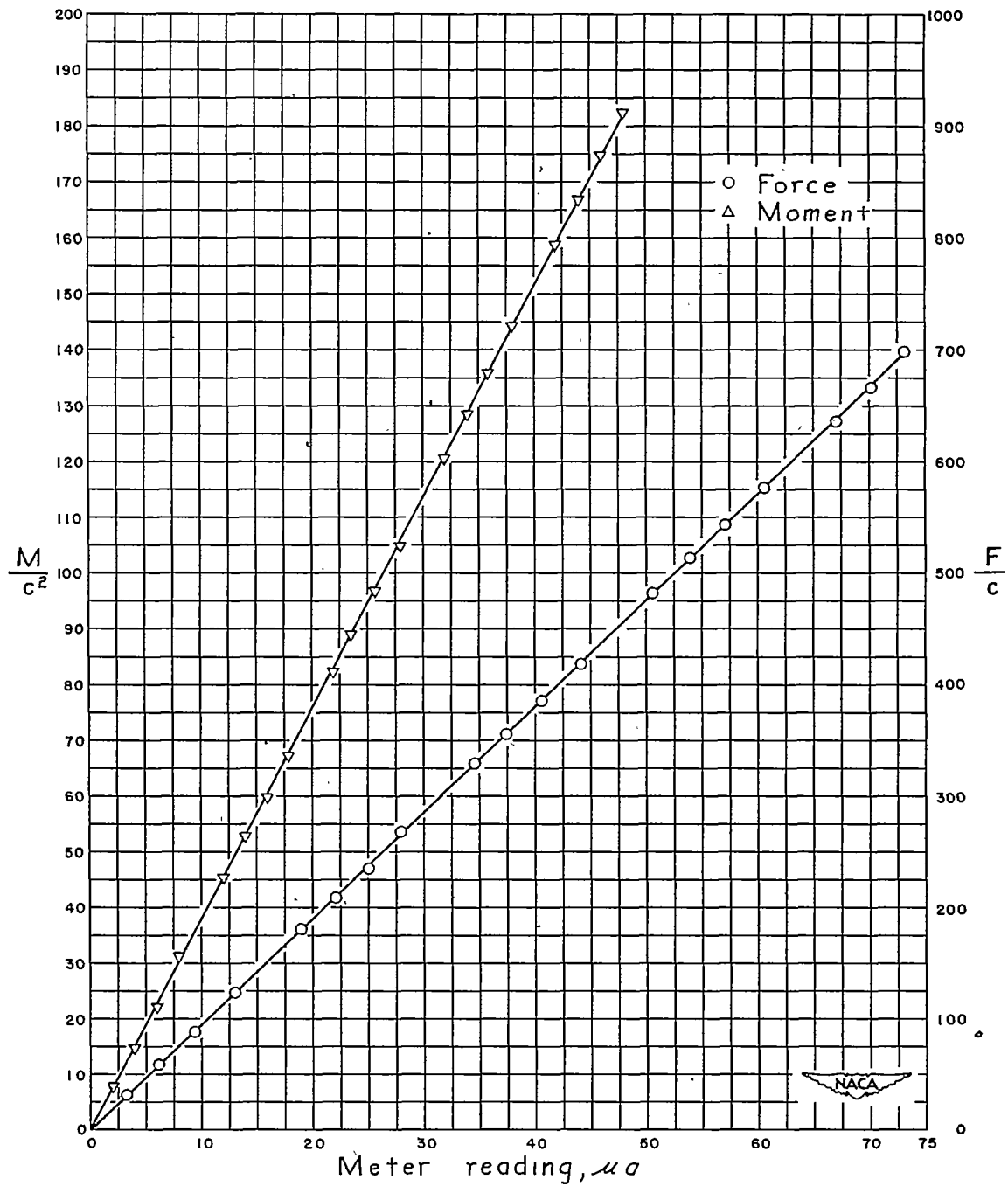
Figure 11.- Calibration curves of model A force and moment integrators.
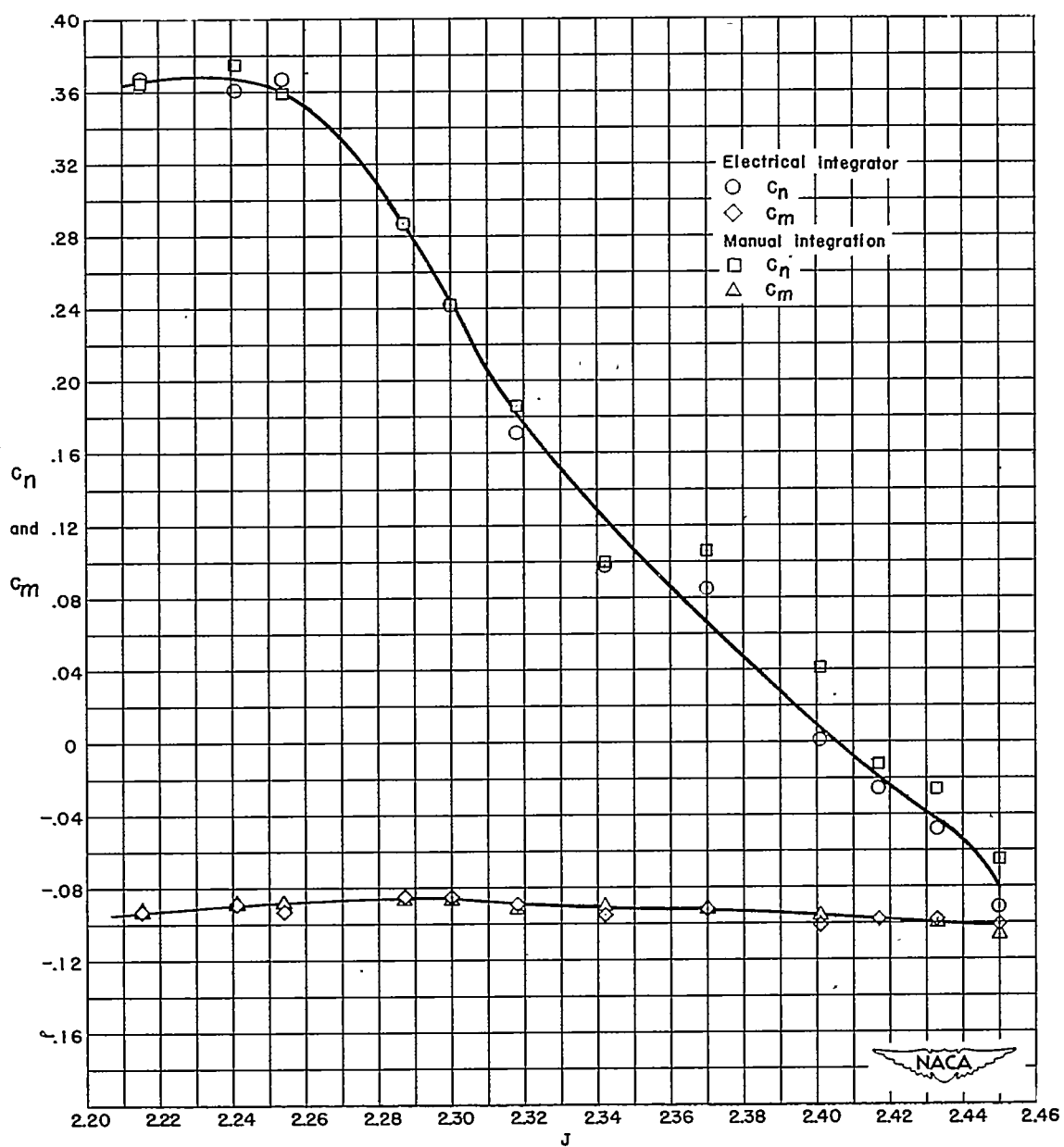
Figure 12.- Advance-diameter ratio against normal-force and moment
coefficients.

Control
panel

c_n
printer

Integrators

c_m
printer

L-68980.1
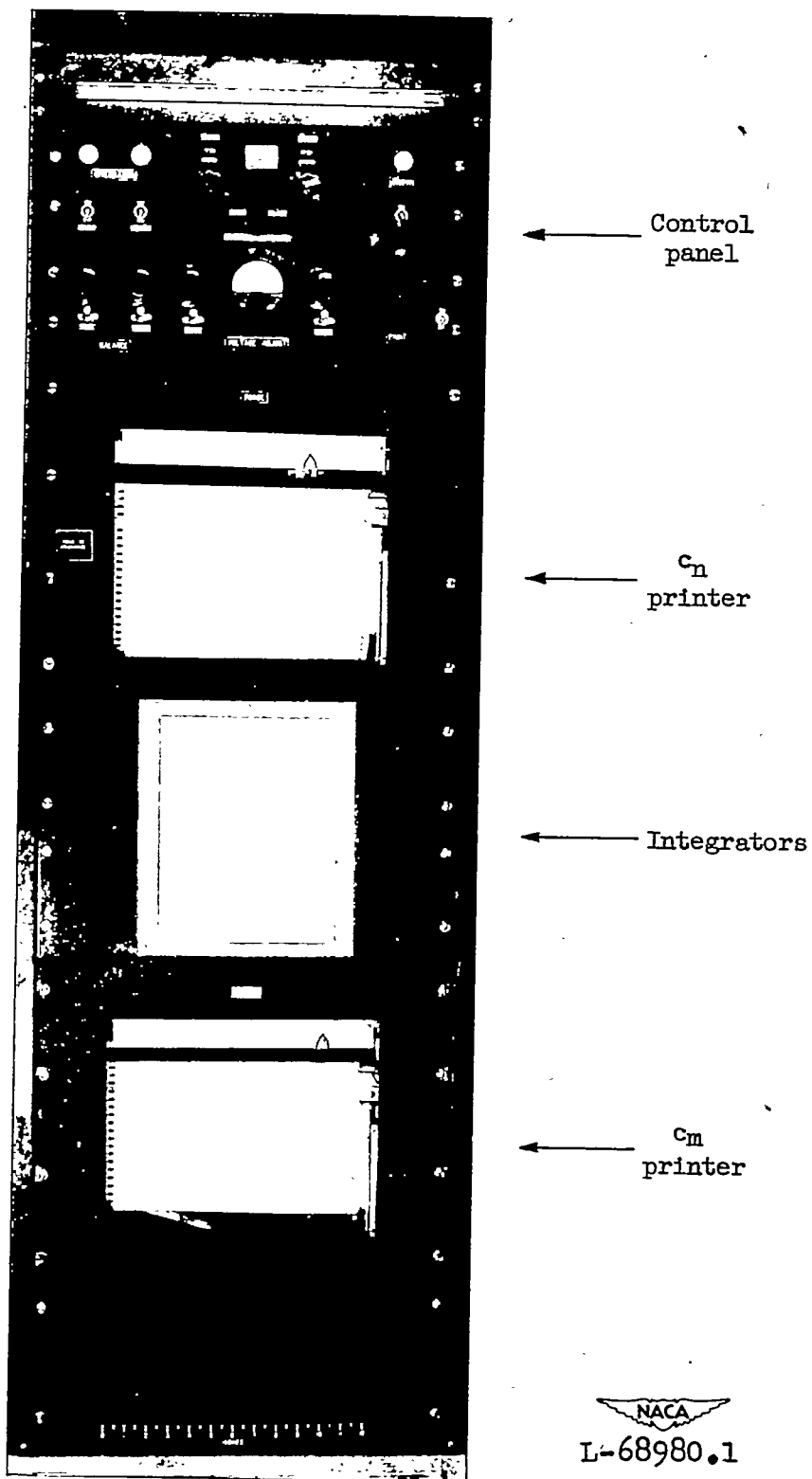
Figure 13.- Front view of model B force and moment integrator.

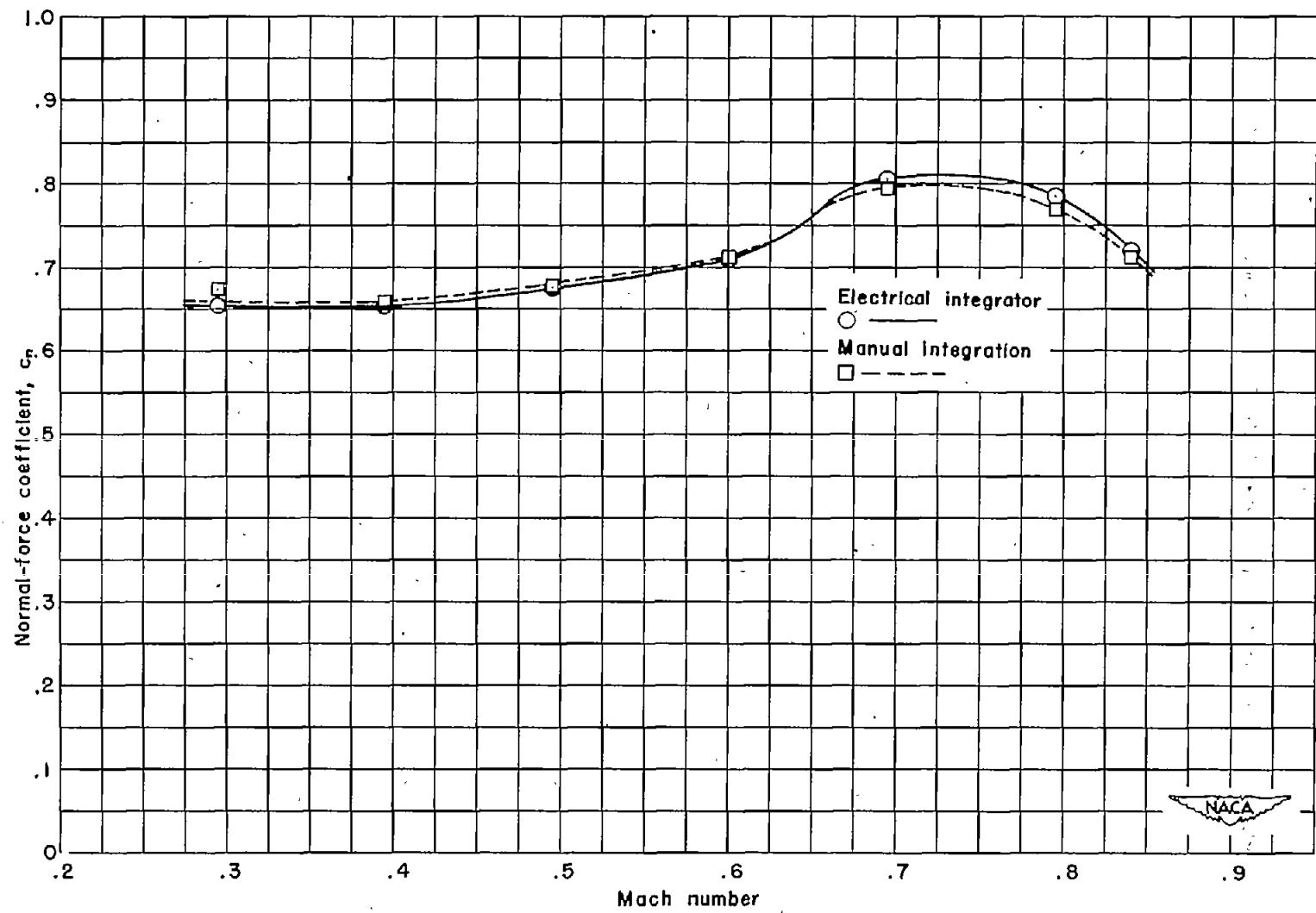Figure 14.- Close-up of control panel of model B force and moment integrator.

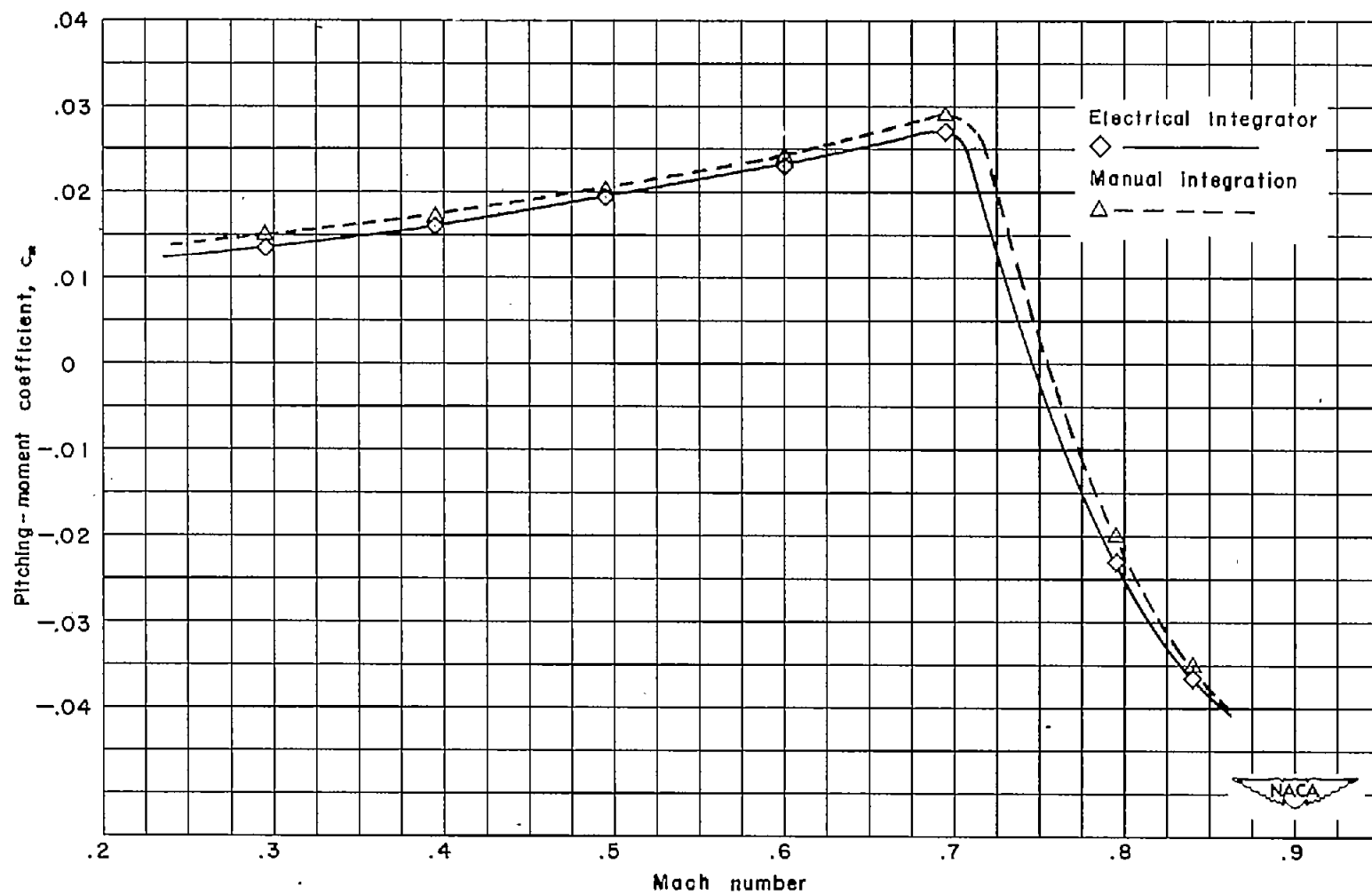Figure 15.- Normal-force coefficient against Mach number.

Figure 16.— Moment coefficient against Mach number.

L-69327

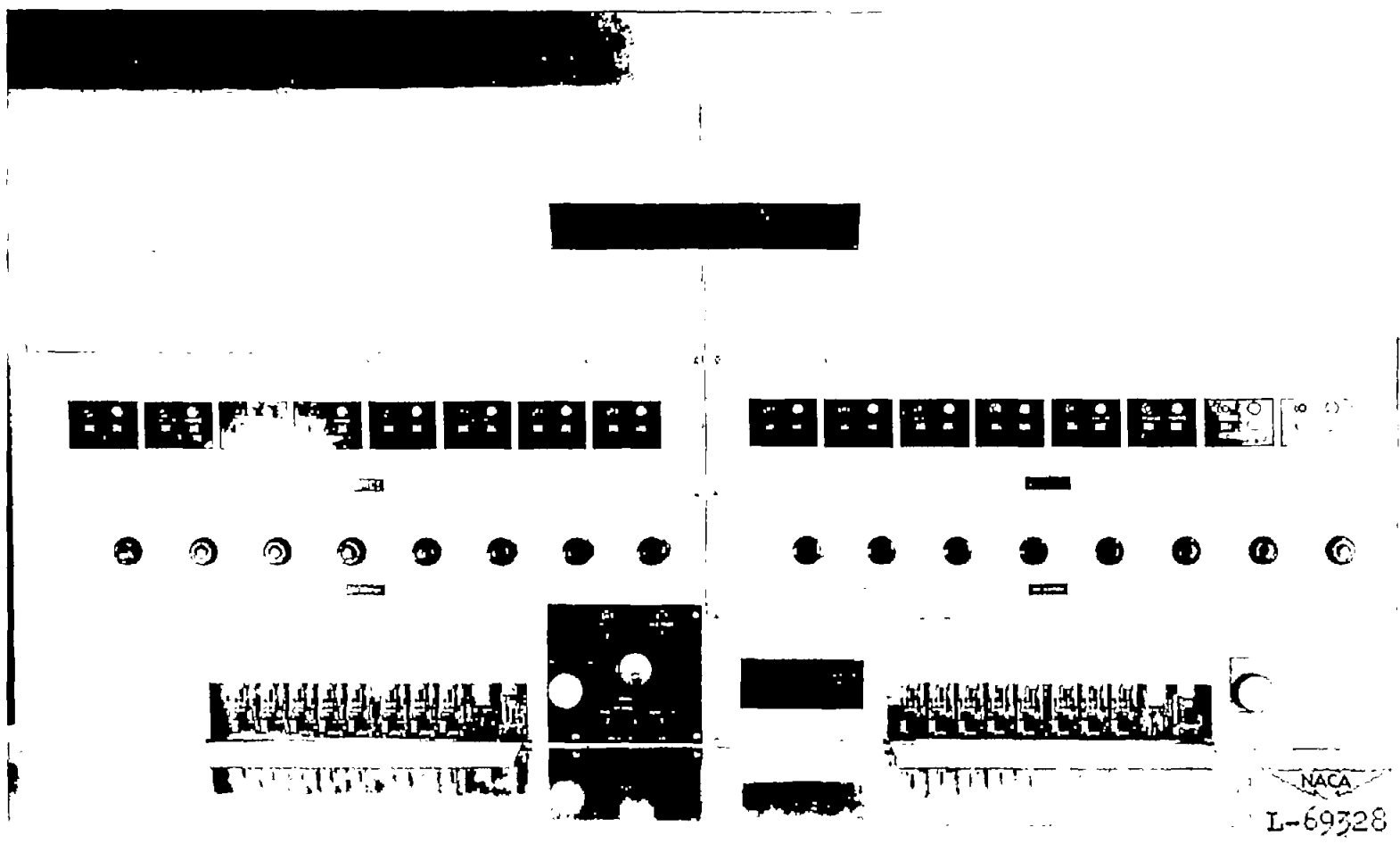Figure 17.- Integrator units of model C force and moment integrator.

Figure 18.- Balance and printer units of model C force and moment integrator.

L-69328